

**Radiobiological effectiveness of iodouracil and the influence of atomic giant resonance**Anuvab Mandal,<sup>1</sup> Madhusree Roy Chowdhury,<sup>1</sup> Chandan Bagdia,<sup>1</sup> Juan M. Monti,<sup>2</sup> Roberto D. Rivarola,<sup>2</sup> P. F. Weck,<sup>3</sup> and Lokesh C. Tribedi<sup>1,\*</sup><sup>1</sup>*Department of Nuclear and Atomic Physics, Tata Institute of Fundamental Research, 1 Homi Bhabha Road, Colaba, Mumbai 400005, India*<sup>2</sup>*Instituto de Física Rosario (CONICET-UNR), Universidad Nacional de Rosario, 2000 Rosario, Argentina*<sup>3</sup>*Sandia National Laboratories, Albuquerque, New Mexico 87185, USA*

(Received 21 April 2020; accepted 12 November 2020; published 14 December 2020)

Hadron therapy combined with nanotechnology has been proposed as an elegant alternative for cancer treatment. Internal amplification of electron emission causing radiobiological effectiveness in nanoinserted biomolecules is of prime importance and has been measured here for the iodouracil molecule. Our experiment involves the measurement of angle and energy resolved double differential cross section (DDCS) of electron emission from iodouracil and uracil (and also water) in collisions with fast  $C^{6+}$  ions. The electron emission from iodouracil is substantially enhanced over that from uracil or water. The enhancement is much larger than the state-of-the-art model for Coulomb ionization based on the continuum distorted wave-eikonal initial state (CDW-EIS) approximation. The electron sensitizing factor ( $\approx 2.4$ ) is in excellent agreement with the strand-breaking sensitizing factor ( $\approx 2.0$ ) for metal nanoparticle embedded in a DNA. The enhancement is explained in terms of collective excitation of strongly correlated 4d electrons, known as atomic giant dipole resonance (GDR) in I atoms. The GDR contribution to the enhancement is derived, which is in excellent agreement with recent theoretical prediction, thereby providing conclusive experimental evidence of the crucial role of collective excitation in radio sensitization.

DOI: [10.1103/PhysRevA.102.062811](https://doi.org/10.1103/PhysRevA.102.062811)**I. INTRODUCTION**

Hadron therapy, which relies on charged-particle beams to treat large cancerous tumors or those resistant to conventional therapies, can be elegantly combined with nanotechnology through the use of nanosensitizers to increase cancer cells' sensitivity toward radiotherapy [1,2]. The study of interaction of the biomolecules and water with fast ions is of immense importance for its application in radiobiology as well as molecular collision physics [3–15]. The high-energy ion-beam induced cancer therapy has the added advantage of delivering a higher dose directly to the target region, in comparison to the conventional photon therapy. A large number of low-energy electrons are emitted in such interaction with biological matter including biomolecules and water. Most of these secondary electrons are emitted near the end of the projectile's trajectory where the energy loss exhibits a peak known as the Bragg peak [16]. It is now well known that the lowest energy electrons (up to about 30 eV) are efficient at breaking the DNA or RNA strands of the cancerous cells through dissociative electron attachment (DEA) [17–20]. A major goal of radiotherapy is to enhance the radiobiological effectiveness, i.e., to generate the same or required amount of damage to the cancerous cells with relatively lower dosage of the ion-beam radiation. Metal nanoparticles (NPs), made of hundreds or thousands of Pt or Au atoms, have been proposed as candidates for radio sensitizers; for example, see, Refs. [21–23]. The most important parameter is the sensitizing factor, i.e., the ratio of

the single-strand break (SSB) (or double-strand break, DSB) event with and without an NP in the DNA.

This factor is closely related to the enhancement of low-energy electron emission in the presence of such inserted atoms. The sensitizing factor or radiobiological effectiveness for the isolated Pt atom attached in a plasmid DNA is found to be  $\approx 1.6$  [21] and that for inserted Au NP is  $\approx 2.0$  [22]. The influence of plasmon excitation to provide enhancement in e-emission has been addressed in experiments involving  $C_{60}$ -fullerene [24–26] as well as in models involving metal nanoparticles by Solovyov and coworkers [2,27]. This model has also predicted enhancements due to the atomic giant resonance (GDR) for which there has not been any quantitative measurement. It was shown that insertion of a 3-nm-diameter Pt NP provides an efficient way to induce lethal damage in DNA. However, the sensitizing effect, in terms of the enhancement of electron yields for such inserted NPs or a metallic atom, has yet to be investigated experimentally. We present here the measurement of the sensitizing factor  $F_S$  using an iodouracil molecule.

The class of 5-halouracil molecules ( $C_4H_3XN_2O_2$ ,  $X = F, Cl, Br, I$ ) are structurally similar to uracil ( $C_4H_4N_2O_2$ ), which is one of the RNA base molecules. Iodouracil is obtained by replacing one of the H atoms of uracil by an I atom. Collision studies using iodouracil (as well as other halouracil molecules) can be enlightening toward the search for a radio sensitizer. A few studies on the low-energy electron induced radio sensitivity through DEA [28–31] are available in the literature. The dehalogenation of halouracils by proton impact has been studied by Champeaux *et al.* [32]. The e-emission spectra from the uracil molecule in collisions with fast protons

\*Corresponding author: [lokesh@tifr.res.in](mailto:lokesh@tifr.res.in)

and bare carbon ions have been studied by Itoh *et al.* [33] and Agnihotri *et al.* [34].

Iodine is known to exhibit atomic giant dipole resonance (GDR) involving the  $4d \rightarrow \epsilon f$  excitation in response to the electromagnetic field [35–39]. Similar GDR has been known to exist also for Xe [40–42] and has been predicted [2] for other metal elements such as Ag, Au, and Pt. The resonance is associated with the collective dipolar oscillatory motion of the entire 4d-shell electrons [35]. Such resonances are strongly damped and decay typically within one period of oscillation [43]. The resonance primarily decays by emission of low-energy electrons. For iodine [39], the GDR occurs at an energy around  $\approx 90$  eV with a width of  $\approx 40$  eV which is also studied in other I-based compounds (i.e.  $\text{CH}_3\text{I}$ ,  $\text{I}_2$ , HI, etc.) [39].

In this article, the e-emission cross sections from 5-iodouracil as well as uracil upon the impact of 5.5-MeV/u C ions are presented. The angular and energy distributions of the e-DDCS ( $d^2\sigma/d\Omega d\epsilon$ ), i.e., ionization cross sections differential in both the solid angle ( $\Omega$ ) and the ejected electron energy ( $\epsilon$ ) are measured. Experimental results are compared with the *ab initio* and state-of-the-art quantum mechanical model based on the continuum distorted wave-eikonal initial state (CDW-EIS) approximation [44]. The total electron emission cross section (TCS), derived by integrating the DDCS over electron energy and emission angles, are also compared with that for the similar results for ionization of water molecule, measured recently.

## II. EXPERIMENTAL PROCEDURE

The details of the experimental techniques are given elsewhere [24,34,45]. In brief, a well-collimated beam of bare C ions with 5.5 MeV/u of energy was obtained from the BARC-TIFR Pelletron accelerator which collided with the targets of iodouracil in a scattering chamber with a base pressure less than  $1 \times 10^{-7}$  mbar. The target was prepared by heating the powder sample in an oven assembly inside the scattering chamber. A nozzle of aspect ratio (length-to-diameter ratio) 10 and of diameter 1.5 mm was used to obtain the effusive vapor jet. The temperature of the oven was raised very slowly, i.e., over a period of  $\approx 24$  hours to  $\approx 120^\circ\text{C}$  to get a sufficient vapor density. Under dry conditions, complete DNA degradation occurs at above  $190^\circ\text{C}$  [46]. Previous studies [32] on fragmentation of different halouracils clearly indicate that there is no thermal decomposition of the sample at  $\approx 120^\circ\text{C}$ . The uniform flow of molecules is ensured by monitoring the deposition rate on a quartz crystal based thickness monitor. The variation in the deposition rate is found to be less than 10%.

The ejected electrons are energy analyzed and detected using an electrostatic hemispherical analyzer with a channel electron multiplier (CEM) detector [47]. A positive voltage of 100 V is applied to the CEM front in order to achieve a uniform detection efficiency ( $\approx 0.9$ ) throughout the detection energy range. The residual electric and magnetic fields, in the interaction region, which were reduced drastically can affect the trajectories of the very-low-energy electrons ( $< 5$  eV). In order to increase the collection efficiency of these electrons, a small preacceleration voltage of 6 V is applied to the entrance and exit apertures of the spectrometer. Additionally,

two  $\mu$ -metal sheets are placed inside the chamber along its inner surface in order to reduce the Earth's magnetic field drastically. The energy resolution of the spectrometer depends mainly on the exit-slit width and the acceptance angle of the entrance slit and is found to be 6% of the detected electron energy.

Electron yields are measured in the range from 1 to 340 eV at different emission angles ranging from  $20^\circ$  to  $160^\circ$ . Background spectra are also recorded. A separate set of experiment was performed with the  $\text{CH}_4$  gas under static pressure condition and the carbon KLL Auger electron spectrum has been used for the normalization to obtain the absolute DDCS values for the iodouracil, as given in Refs. [24,34,45]. The total uncertainty in the deduction of the absolute values of the DDCS is  $\approx 25$ –30%, primarily arising from the vapor density fluctuation  $\approx 10\%$ , the normalization procedure (15–18%), the statistical uncertainty ( $\approx 5\%$ ), solid-angle path length (8–10%), etc.

## III. THEORETICAL DESCRIPTION

An independent particle approximation is employed to describe the single ionization reaction. The treatment of the case of atomic targets [48] is extended to the case of molecular ones. It means that only one electron of each one of the molecular orbitals is considered to be promoted to a continuum state whereas all the other target electrons (the passive electrons) are considered to remain as frozen in their initial states. This procedure is then applied to each one of the molecular orbitals. The dynamics of the process is described within the prior form of the continuum distorted wave-eikonal initial state (CDW-EIS) formalism. The straight line version of the impact parameter approximation is used for the calculations [49].

The interest is focused only in the spectra of the final ejected electron parameters (energy and angle), considering that the contribution of all molecular orientations are averaged. Thus, it is assumed that the interaction between the projectile and the passive electrons does not affect the ionization process itself and the corresponding potentials can be eliminated from the total electronic Hamiltonian [48].

Into the CDW-EIS model the initial and final distorted wave functions for each one of the molecular orbitals are chosen as

$$\chi_i^+ = \varphi_i \exp\left[-i\frac{Z_P}{v} \ln(vs + \vec{v} \cdot \vec{s})\right] \exp(-i\epsilon_j t) \quad (1)$$

and

$$\begin{aligned} \chi_f^+ &= \varphi_f(\vec{x}) N^*(Z_T^*/k) {}_1F_1(-iZ_T^*/k, 1; -ikx - i\vec{k} \cdot \vec{x}) \\ &\times N^*(Z_P/p) {}_1F_1(-iZ_P/p, 1; -ips - i\vec{p} \cdot \vec{s}) \\ &\times \exp\left(-i\frac{k^2}{2}t\right). \end{aligned} \quad (2)$$

In these equations,  $\varphi_i$  and  $\varphi_f$  are the initial orbital and final plane-wave functions. The vectors  $\vec{x}$  and  $\vec{s}$  are the position of the electron with respect to the target nucleus and projectile respectively, and  $\epsilon_j$  is the initial orbital energy of the  $j$ -molecular orbital. Also,  $\vec{v}$  is the collision velocity,  $\vec{k}$  and  $\vec{p} = \vec{k} - \vec{v}$  are the momentum of the electron with respect to the target and projectile respectively, with  $Z_P$  being the

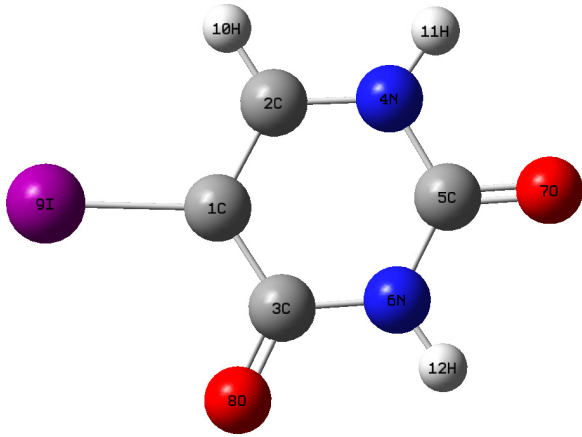


FIG. 1. A geometrical representation of the ground-state equilibrium structure of the 5-iodouracil.

projectile nuclear charge and  $Z_T^*$  being an effective target nuclear charge to describe the interaction of the active electron with the residual target with an effective Coulomb potential.  $N(a) = \exp(\pi a/2)\Gamma(1 - ia)$  with  $Z_T^*/k$  and  $Z_p/p$  are normalization factors, with  $\Gamma$  representing the Gamma function.

In order to describe  $\varphi_i$ , each molecular orbital was expressed as a linear combination of the atomic orbitals (LCAO). A geometrical representation of the ground-state equilibrium structure of the 5-iodouracil molecule is given in Fig. 1. The atoms are labeled with a number that allows us to identify which of them correspond to each one of the different molecular orbitals. *Ab initio* calculations were performed in the gas phase using the restricted Hartree-Fock (RHF) method implemented in the GAUSSIAN 09 software [50]. The C, O, H, and N atoms were represented using Pople's split-valence triple-zeta basis set 6-311G, while iodine was described using a Douglas-Kroll-Hess (DKH) contracted Gaussian basis set of triple zeta valence quality plus polarization functions (TZP), including explicitly all electrons and scalar relativistic effects [51]. The resulting ionization energy is 9.69 eV, which is very close to the 9.93-eV experimental value.

No symmetry constraints were applied in the relaxation calculation; the resulting equilibrium structure of the iodouracil molecule adopts the Cs point group symmetry (mirror plane). A population analysis of all occupied orbitals was carried out using the self-consistent field (SCF) density, with the minimum contribution percentage to include in individual orbital population analysis set to 1%. For each  $j$ -molecular orbital, the effective number of  $\xi_{j,i}$  electrons, relative to the atomic component  $i$ , was obtained from a standard Mulliken population analysis. Then, taken into account that experimentally the orientation of the molecular target is not distinguished, an average over all initial positions appears as necessary. In order to simulate this average, all atomic compounds of the molecular orbitals are considered centered on a unique center, but preserving the corresponding population analysis described above. Thus, the calculation for the different target orientations is avoided. This approximation has been previously employed with success to describe the existing experimental spectra for ionization and electron capture in ion impact on DNA nucleobases and Uracil (see, for example,

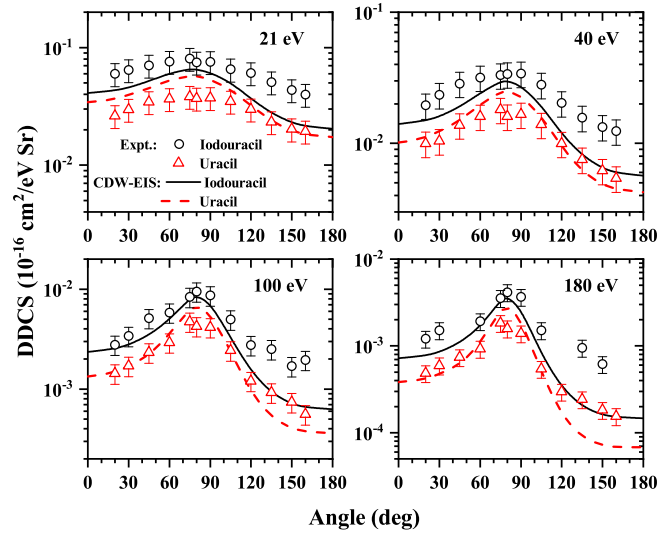


FIG. 2. Angular dependence of DDCS of electron emission from 5-iodouracil and uracil induced by 5.5-MeV/u  $C^{6+}$  ions.

Refs. [52,53]). The final continuum wave function associated with each one of the atomic components of the different molecular orbitals is described using an effective target charge  $Z_T^* = Z_{ji} = (-2n_{ji}^2\varepsilon_j)^{1/2}$ , where  $n_{ji}$  is the principal quantum number corresponding to the quantum state of the considered atom.

Proceeding in the same way as Galassi *et al.* [53], we obtained double differential cross sections  $d^2\sigma_j/d\Omega d\epsilon$  corresponding to each molecular orbital, as a function of the energy  $\epsilon$  and the solid angle  $\Omega$  subtended by the ejected electron, using the expression

$$\frac{d^2\sigma_j}{d\Omega d\epsilon} = \sum_{i=1}^{N_j} \xi_{ji} \frac{d^2\sigma_{ji}}{d\Omega d\epsilon}, \quad (3)$$

where  $\xi_{ji}$  corresponds to the population of the  $i$  atomic component of the  $j$  molecular orbital and  $d^2\sigma_{ji}/d\Omega d\epsilon$  represents the double differential cross section for ionization of this atom.  $N_j$  is the total number of the atomic components of each  $j$  molecular orbital. Then, the double differential cross section of the complete molecule can be calculated summing over all molecular orbital contributions,

$$\frac{d^2\sigma}{d\Omega d\epsilon} = \sum_{j=1}^N \frac{d^2\sigma_j}{d\Omega d\epsilon}. \quad (4)$$

In this equation,  $N$  is the total number of molecular orbitals. Population and binding energies of the uracil molecular orbitals as well as a representation of their equilibrium geometries were given in Galassi *et al.* [53].

#### IV. RESULTS AND DISCUSSION

The angular dependence of the observed DDCS are plotted and compared with the values calculated from the CDW-EIS model at four selected energies (i.e., 21, 40, 100, and 180 eV) in Fig. 2. The observed data show broad peaks around  $80^\circ$  at all the energies and such a peaking behavior is well explained

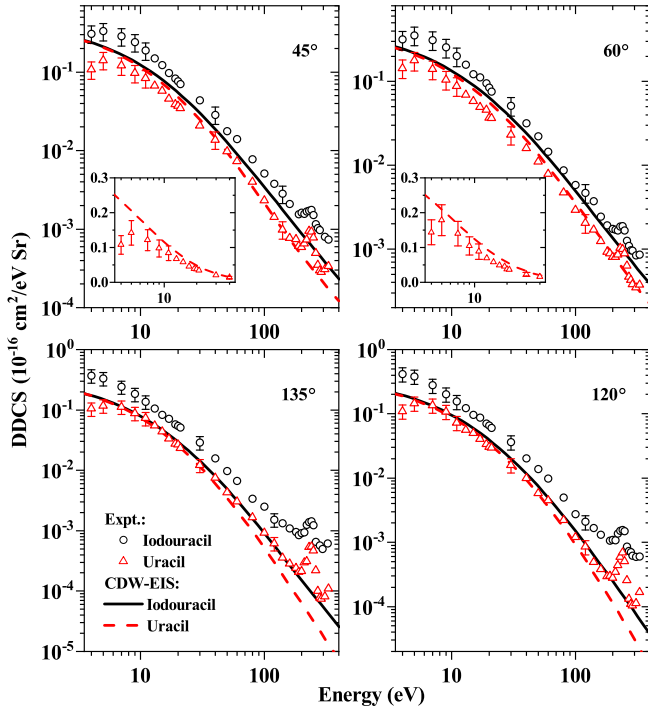


FIG. 3. Energy dependence of DDCS of electron emission from 5-iodouracil and uracil induced by 5.5-MeV/u  $C^{6+}$  ions. The DDCS below 40 eV for uracil at forward angles are shown in insets.

in terms of binary-collision mechanism in ion-atom collisions. Accordingly, the behavior is consistent with the CDW-EIS model as shown in Fig. 2.

Ejected energy dependence of the e-DDCS for the iodouracil and uracil at four different emission angles are shown in Fig. 3. The DDCS spectra starting from a few eV to 330 eV are displayed. The carbon KLL Auger electron peak is observed at  $\approx 240$  eV. The DDCS spectra show a rapid decrease, i.e., by  $\approx 3$  orders of magnitudes, with the increasing electron energy (cf. Fig. 3) indicating the dominant contribution of the low-energy electrons. For iodouracil the experiment-theory agreement is not so good, but for uracil the agreement is reasonably good. In particular, the model (dashed lines) explains the uracil data quite well for backward angles over the whole energy range. For the forward angles, the theory agrees with the data quite well above 30 eV. Even at lower energies, the calculations fall slightly higher than the data but remain within experimental uncertainties. To explain this, we have used two insets (for the forward angles) in which the low-energy data (up to 40 eV) are plotted for uracil. The larger disagreement with the iodouracil data, particularly at lower energies in the case of forward angles, is interesting since this energy range is quite important for the hadron therapy. This different could be related to the atomic GDR which is not included in the model calculation (see below). The angular dependence of the iodouracil-to-uracil DDCS ratio is plotted in Fig. 4(a). The CDW-EIS model underestimates the DDCS ratio values at all four energies. The observed energy dependence of iodouracil-to-uracil DDCS ratios are plotted in Fig. 4(b) for fixed emission angles. The enhancement of e-DDCS is found to be almost independent

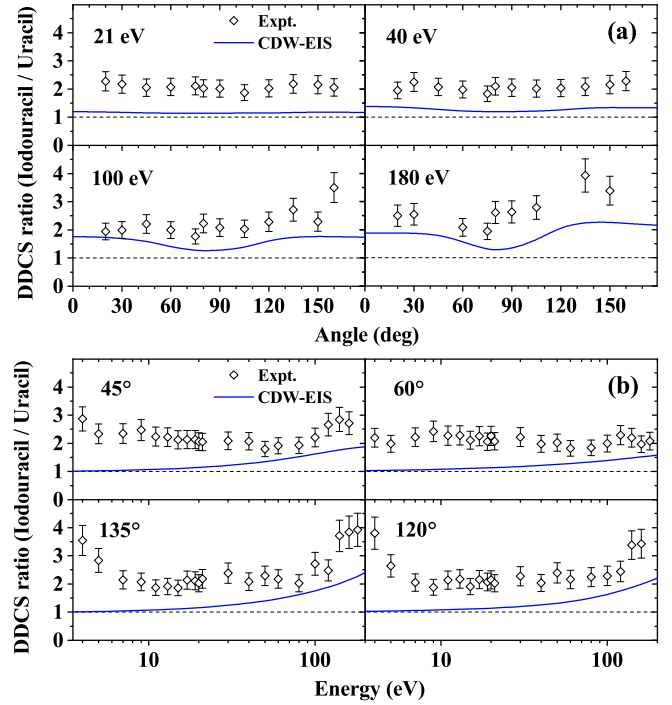


FIG. 4. (a) Angle and (b) energy dependence of the DDCS ratio of iodouracil to uracil. The dashed lines represent the ratio value of one.

of e-emission angle. The average ratios at the forward and backward angles are about 2.3. This implies that the introduction of the I atom in the uracil molecule enhances the e-emission from iodouracil substantially, giving rise to sensitizing factor  $F_S^{el} \approx 2.3$ . However, according to the CDW-EIS model which includes all the orbitals (29 for uracil and 55 for iodouracil), the calculated (Fig. 5) ratio is less than 1.05 for around 3 eV. Then it increases to about 1.05–1.10 for 10 eV, 1.10–1.15 for 15 eV, and 1.15–1.23 for 25 eV. For 30 eV energy, this ratio is between 1.17 to 1.30. An average enhancement of  $f_{ionz} \approx 1.15$  is estimated for the energy range of 1 to 30 eV, which is relevant for the present purpose. Therefore, experimentally measured  $F_S^{el} \approx 2.3$  cannot be explained in terms of the CDW-EIS based on independent electron approximation. The Auger cascade can contribute only little, i.e.,  $\approx 12\%$ , considering only the  $N_{4,4}OO$  Auger lines [54], giving the Auger factor  $f_A \approx 1.12$

The atomic GDR of the  $4d$  electrons decays by the emission of the low-energy electrons, causing an enhancement

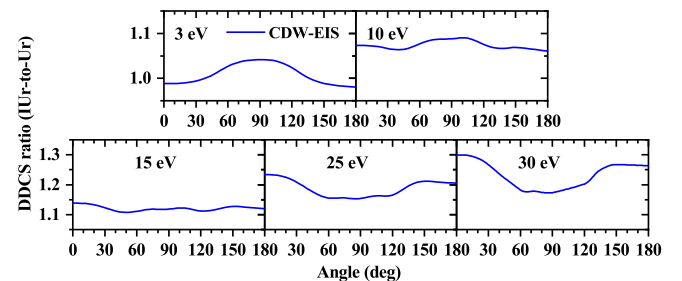


FIG. 5. Angle dependence of the theoretical DDCS ratio of iodouracil to uracil in low emission energies.

as predicted in Refs. [2,27]. The GDR induced enhancement  $f_{GDR}$  is thereby derived from the total enhancement as,  $2.3/(f_{ionz} \cdot f_A)$ , i.e.,  $f_{GDR} \approx 1.8$ . This is also close to the observed enhancement due to collective plasmon excitation in  $C_{60}$  fullerene for which the enhancement factor was about 1.5 [24,55,56]. In the present study, any structure in the electron DDCS spectrum due to the deexcitation of the GDR (with energy  $E_{GDR}$ ) is not visible. Such electron peak should appear at an energy lower than  $E_{GDR}$  since some energy must be spent to ionize these bound electrons. The width of the GDR peak (i.e., about 40 eV) is too large for the resonance to be observable on top of the steep energy dependence of the DDCS.

The measured TCS for iodouracil and uracil are  $8.51 \times 10^{-15}$  and  $4.44 \times 10^{-15}$  cm<sup>2</sup>, respectively. To understand the radio-sensitizing effect one important aspect is to compare the DDCS or TCS with that for the water molecule, since water constitutes about 60% of the human body. The TCS for e-emission from iodouracil is found to be  $\approx 15$  times larger than that for a water molecule having a TCS,  $\approx 5.6 \times 10^{-16}$  cm<sup>2</sup> [57]. If one normalizes the TCS for the equal volume of water and iodouracil, then the sensitizing factor ( $F_S^{el}$ ) becomes  $15/6 = 2.5$  since the volume of iodouracil is six times larger than that of the water molecule. However, the theoretical (CDW-EIS) prediction [14], based on Coulomb ionization alone, for the iodouracil-to-water molecule ratio [ $f_{ionz}$ ] is only 6.2 [=  $5.47 \times 10^{-15}$  cm<sup>2</sup>/ $8.8 \times 10^{-16}$  cm<sup>2</sup>] and  $\approx 1.0$  based on the volume-normalization. Assuming the rest of the e-emission process is mostly governed by the GDR in I atom (apart from Auger cascade) one again obtains the GDR contribution as  $f_{GDR} = 15/(6.2f_A)$ , i.e., about  $2.20 \pm 0.44$  (which is independent of single molecule since molecules of same volume are considered). This value is in excellent agreement with that derived above, i.e.,  $1.80 \pm 0.36$  from the iodouracil-to-uracil ratio. Since they are very close to each other one may use an average value of  $f_{GDR} \approx 2.0$ . It may also be noted that the sensitizing factor  $F_S^{sb}$ , measured from the DNA strand-breaking statistics, for an isolated Pt atom embedded in a plasmid DNA was found to be quite close, i.e.,  $\approx 1.6$  [21] and that for an inserted Au NP of bigger size was  $\approx 2.0$  [22], again in excellent agreement with the measured  $F_S^{el}$  of  $2.3 \pm 0.5$  between an iodouracil and uracil and 2.5 between iodouracil and water. We may therefore conclude that  $F_S^{sb} \sim F_S^{el}$ .

To get insight into the derived value of  $f_{GDR}$  ( $\approx 2.0$ ) involving iodine, we may refer to the predicted values [2] for the Ag atom. In both the atoms, all 10 electrons in the  $4d$ -subshell contribute to the atomic GDR. However, in real application with nanoparticle (NP) inserted in a DNA a large number of atoms are involved. For example, in the case of the Ag NP of diameter 1 nm the predicted enhancement (over water of same volume) was about 15 to 30 times in the e-energy range of 0 to 25 eV due to the atomic GDR excited by protons of velocity ( $v$ ) 6.35 a.u. This implies an enhancement of a factor of  $\approx 1.0$  to 2.0 (over 0 to 25 eV) per Ag atom since the

number of contributing Ag atoms were about 1/3 of the total of 40 atoms [58] in the NP based on the impact parameter ( $b$ ) consideration [2]. This enhancement was re-estimated for the present collision velocity using the scaling approach. At  $v \approx 15$  a.u., the range of  $b$  and therefore the fraction of Ag atoms contributing to the GDR increases to about 85–90%. The reduction in the GDR cross section was also accounted for by using Eqs. (18) and (19) in Ref. [27]. Finally, the reduction in the TCS of water was also considered using the  $v^{-1.7}$  scaling rule [57]. Thus, the enhancement per Ag atom over water would be a factor of  $\approx 3.0$  [2,27,58] at 25 eV. Therefore, over the e-energy 0 to 25 eV, this factor will be 1.5 to 3.0, giving an average value of  $f_{GDR}^{Ag} \approx 2.25$ . This value is in excellent agreement to that derived  $f_{GDR}^I \approx 2.0 \pm 0.4$  for the I atom and thereby confirming the theoretical prediction on the GDR contribution to the sensitizing effect.

## V. CONCLUSIONS

In conclusion, the DDCS and TCS of e-emission from iodouracil and uracil upon the bombardment of 5.5-MeV/u bare C ions have been measured. The measured radio-sensitizing or electron enhancement factors of 2.3 and 2.5 over uracil and water, respectively, are in excellent agreement with the radio-sensitizing factors measured in the case of Pt or Au NP embedded in a DNA from the strand-breaking studies. The enhancement is substantially large compared to the prediction of the state-of-the-art CDW-EIS model but the atomic GDR of the strongly correlated  $4d$  electrons in the I atom is shown to play a crucial role. The GDR contribution provides an enhancement of a factor of  $2.0 \pm 0.4$ , which is in excellent agreement with the theoretical prediction based on the GDR in an atom with filled  $4d$  subshell (such as Ag). This provides conclusive experimental evidence of the crucial role of the collective excitation in radio sensitization. It is evident that introduction of a single halogen atom, I, in the biomolecule, can indeed cause a substantial nanosensitizing effect. Therefore, the halouracil molecules, in particular, iodouracil, may have potential as a prototypical system for the radio sensitizer, provided it satisfies other practical considerations.

## ACKNOWLEDGMENTS

The authors thank the staff of the BARC-TIFR Pelletron accelerator facility and A. Verkhovtsev and A. Solovyov for communications about their published work. Sandia National Laboratories is a multimission laboratory managed and operated by National Technology and Engineering Solutions of Sandia, LLC, a wholly owned subsidiary of Honeywell International, Inc., for the US Department of Energy's National Nuclear Security Administration under Contract No. DE-NA0003525. The views expressed in the article do not necessarily represent the views of the US DOE or the US Government.

[1] E. Porcel, S. Liehn, H. Remita, N. Usami, K. Kobayashi, Y. Furusawa, C. L. Sech, and S. Lacombe, *Nanotechnology* **21**, 085103 (2010).

[2] A. V. Verkhovtsev, A. V. Korol, and A. V. Solov'yov, *Phys. Rev. Lett.* **114**, 063401 (2015).

- [3] P. Håkansson, E. Jayasinghe, A. Johansson, I. Kamensky, and B. Sundqvist, *Phys. Rev. Lett.* **47**, 1227 (1981).
- [4] B. Coupier, B. Farizon, M. Farizon, M. J. Gaillard, F. Gobet, N. V. de Castro Faria, G. Jalbert, S. Ouaskit, M. Carré, B. Gstir, G. Hanel, S. Denifl, L. Feketeova, P. Scheier, and T. D. Märk, *Eur. Phys. J. D* **20**, 459 (2002).
- [5] J. Tabet, S. Eden, S. Feil, H. Abdoul-Carime, B. Farizon, M. Farizon, S. Ouaskit, and T. Märk, *Int. J. Mass Spectrometry* **292**, 53 (2010).
- [6] Y. Iriki, Y. Kikuchi, M. Imai, and A. Itoh, *Phys. Rev. A* **84**, 052719 (2011).
- [7] A. N. Agnihotri, S. Kasthurirangan, S. Nandi, A. Kumar, M. E. Galassi, R. D. Rivarola, O. Fojón, C. Champion, J. Hanssen, H. Lekadir, P. F. Weck, and L. C. Tribedi, *Phys. Rev. A* **85**, 032711 (2012).
- [8] A. N. Agnihotri, S. Kasthurirangan, S. Nandi, A. Kumar, C. Champion, H. Lekadir, J. Hanssen, P. F. Weck, M. E. Galassi, R. D. Rivarola, O. Fojón, and L. C. Tribedi, *J. Phys. B: At., Mol. Opt. Phys.* **46**, 185201 (2013).
- [9] L. C. Tribedi, A. N. Agnihotri, M. E. Galassi, R. D. Rivarola, and C. Champion, *Eur. Phys. J. D* **66**, 303 (2012).
- [10] M. A. Bolorizadeh and M. E. Rudd, *Phys. Rev. A* **33**, 888 (1986).
- [11] M. E. Rudd, T. V. Goffe, R. D. DuBois, and L. H. Toburen, *Phys. Rev. A* **31**, 492 (1985).
- [12] L. H. Toburen, W. E. Wilson, and R. J. Popowich, *Radiat. Res.* **82**, 27 (1980).
- [13] C. Dal Cappello, C. Champion, O. Boudrioua, H. Lekadir, Y. Sato, and D. Ohsawa, *Nucl. Instr. Meth. Phys. Res. B* **267**, 781 (2009).
- [14] S. Bhattacharjee, S. Biswas, J. M. Monti, R. D. Rivarola, and L. C. Tribedi, *Phys. Rev. A* **96**, 052707 (2017).
- [15] S. Bhattacharjee, S. Biswas, C. Bagdia, M. Roychowdhury, S. Nandi, D. Misra, J. M. Monti, C. A. Tachino, R. D. Rivarola, C. Champion, and L. C. Tribedi, *J. Phys. B At. Mol. Opt. Phys.* **49**, 065202 (2016).
- [16] G. F. Knoll, *Radiation Detection and Measurement*, 3rd ed. (Wiley, New York, 2000), Chap. 2, p. 32.
- [17] B. Boudaïffa, P. Cloutier, D. Hunting, M. A. Huels, and L. Sanche, *Science* **287**, 1658 (2000).
- [18] S. Gohlke, A. Rosa, E. Illenberger, F. Brüning, and M. A. Huels, *J. Chem. Phys.* **116**, 10164 (2002).
- [19] H. Abdoul-Carime, S. Gohlke, and E. Illenberger, *Phys. Rev. Lett.* **92**, 168103 (2004).
- [20] C. König, J. Kopyra, I. Bald, and E. Illenberger, *Phys. Rev. Lett.* **97**, 018105 (2006).
- [21] E. Porcel, O. Tillement, F. Lux, P. Mowat, N. Usami, K. Kobayashi, Y. Furusawa, C. L. Sech, S. Li, and S. Lacombe, *Nanomedicine: Nanotechnol., Biol. Med.* **10**, 1601 (2014).
- [22] K. T. Butterworth, J. A. Wyer, M. Brennan-Fournet, C. J. Latimer, M. B. Shah, F. J. Currell, and D. G. Hirst, *Radiat. Res.* **170**, 381 (2008).
- [23] F. Xiao, Y. Zheng, P. Cloutier, Y. He, D. Hunting, and L. Sanche, *Nanotechnology* **22**, 465101 (2011).
- [24] A. H. Kelkar, L. Gulyás, and L. C. Tribedi, *Phys. Rev. A* **92**, 052708 (2015).
- [25] A.H. Kelkar, D. Misra, L. Gulyas, and L.C. Tribedi, *Eur. Phys. J. D* **74**, 157 (2020).
- [26] A. V. Verkhovtsev, A. V. Korol, A. V. Solov'yov, P. Bolognesi, A. Ruocco, and L. Avaldi, *J. Phys. B: At. Mol. Opt. Phys.* **45**, 141002 (2012).
- [27] A. V. Verkhovtsev, A. V. Korol, and A. V. Solov'yov, *J. Phys. Chem. C* **119**, 11000 (2015).
- [28] H. Abdoul-Carime, M. A. Huels, F. Brüning, E. Illenberger, and L. Sanche, *J. Chem. Phys.* **113**, 2517 (2000).
- [29] M.-A. Herve du Penhoat, M. A. Huels, P. Cloutier, J.-P. Jay-Gerin, and L. Sanche, *Phys. Chem. Chem. Phys.* **5**, 3270 (2003).
- [30] H. Abdoul-Carime, M. A. Huels, E. Illenberger, and L. Sanche, *Int. J. Mass Spectr.* **228**, 703 (2003).
- [31] D. V. Klyachko, M. A. Huels, and L. Sanche, *Rad. Res.* **151**, 177 (1999).
- [32] J.-P. Champeaux, P. Carcabal, J. Rabier, P. Cafarelli, M. Sence, and P. Moretto-Capelle, *Phys. Chem. Chem. Phys.* **12**, 5454 (2010).
- [33] A. Itoh, Y. Iriki, M. Imai, C. Champion, and R. D. Rivarola, *Phys. Rev. A* **88**, 052711 (2013).
- [34] A. N. Agnihotri, S. Nandi, S. Kasthurirangan, A. Kumar, M. E. Galassi, R. D. Rivarola, C. Champion, and L. C. Tribedi, *Phys. Rev. A* **87**, 032716 (2013).
- [35] G. Wendin, *J. Phys. B* **6**, 42 (1973).
- [36] D. W. Lindle, P. H. Kobra, C. M. Truesdale, T. A. Ferrett, P. A. Heimann, H. G. Kerkhoff, U. Becker, and D. A. Shirley, *Phys. Rev. A* **30**, 239 (1984).
- [37] A. P. Hitchcock and C. E. Brion, *J. Elec. Spectr. Rel. Phenomena* **13**, 193 (1978).
- [38] F. J. Comes, U. Nielsen, and W. H. E. Schwarz, *J. Chem. Phys.* **58**, 2230 (1973).
- [39] L. Nahon, A. Svensson, and P. Morin, *Phys. Rev. A* **43**, 2328 (1991).
- [40] D. L. Ederer, *Phys. Rev. Lett.* **13**, 760 (1964).
- [41] U. Becker, T. Prescher, E. Schmidt, B. Sonntag, and H. E. Wetzel, *Phys. Rev. A* **33**, 3891 (1986).
- [42] B. Kammerling, H. Kossman, and V. Schmidt, *J. Phys. B At. Mol. Opt. Phys.* **22**, 841 (1989).
- [43] J.-P. Connerade, J.-M. Esteva, and R. Karnatak, editors, *Giant Resonances in Atoms, Molecules, and Solids* (Springer, New York, 1987).
- [44] P. D. Fainstein, L. Gulyás, F. Martín, and A. Salin, *Phys. Rev. A* **53**, 3243 (1996).
- [45] S. Bhattacharjee, C. Bagdia, M. R. Chowdhury, A. Mandal, J. M. Monti, R. D. Rivarola, and L. C. Tribedi, *Phys. Rev. A* **100**, 012703 (2019).
- [46] M. Karni, D. Zidon, P. Polak, Z. Zalevsky, and O. Shefi, *DNA and Cell Biology* **32**, 298 (2013).
- [47] D. Misra, K. V. Thulasiram, W. Fernandes, A. H. Kelkar, U. Kadhane, A. Kumar, Y. Singh, L. Gulyás, and L. C. Tribedi, *Nucl. Instr. Meth. Phys. Res. B* **267**, 157 (2009).
- [48] P. D. Fainstein, V. H. Ponce, and R. D. Rivarola, *J. Phys. B At. Mol. Opt. Phys.* **21**, 287 (1988).
- [49] S. E. Corchs, R. D. Rivarola, and J. H. McGuire, *Phys. Rev. A* **47**, 3937 (1993).
- [50] M. J. Frisch, G. W. Trucks, H. B. Schlegel, G. E. Scuseria, M. A. Robb, J. R. Cheeseman, G. Scalmani, V. Barone, B. Mennucci, G. A. Petersson, H. Nakatsuji, M. Caricato, X. Li, H. P. Hratchian, A. F. Izmaylov, J. Bloino, G. Zheng, J. L.

- Sonnenberg, M. Hada, M. Ehara, K. Toyota, R. Fukuda, J. Hasegawa, M. Ishida, T. Nakajima, Y. Honda, O. Kitao, H. Nakai, T. Vreven, J. A. Montgomery Jr., J. E. Peralta, F. Ogliaro, M. Bearpark, J. J. Heyd, E. Brothers, K. N. Kudin, V. N. Staroverov, R. Kobayashi, J. Normand, K. Raghavachari, A. Rendell, J. C. Burant, S. S. Iyengar, J. Tomasi, M. Cossi, N. Rega, J. M. Millam, M. Klene, J. E. Knox, J. B. Cross, V. Bakken, C. Adamo, J. Jaramillo, R. Gomperts, R. E. Stratmann, O. Yazyev, A. J. Austin, R. Cammi, C. Pomelli, J. W. Ochterski, R. L. Martin, K. Morokuma, V. G. Zakrzewski, G. A. Voth, P. Salvador, J. J. Dannenberg, S. Dapprich, A. D. Daniels, À. Farkas, J. B. Foresman, J. V. Ortiz, J. Cioslowski, and D. J. Fox, *Gaussian 09 rev. A.02* (Gaussian, Wallingford, CT, 2009).
- [51] F. E. Jorge, A. Canal Neto, G. G. Camiletti, and S. F. Machado, *J. Chem. Phys.* **130**, 064108 (2009).
- [52] C. Champion, P. F. Weck, H. Lekadir, M. E. Galassi, O. A. Fojón, P. Abufager, R. D. Rivarola, and J. Hanssen, *Phys. Med. Biol.* **57**, 3039 (2012).
- [53] M. E. Galassi, C. Champion, P. F. Weck, R. D. Rivarola, O. Fojón, and J. Hanssen, *Phys. Med. Biol.* **57**, 2081 (2012).
- [54] L. O. Werme, T. Bergmark, and K. Siegbahn, *Phys. Scr.* **6**, 141 (1972).
- [55] S. Cheng, H. G. Berry, R. W. Dunford, H. Esbensen, D. S. Gemmell, E. P. Kanter, T. LeBrun, and W. Bauer, *Phys. Rev. A* **54**, 3182 (1996).
- [56] H. Tsuchida, A. Itoh, K. Miyabe, Y. Bitoh, and N. Imanishi, *J. Phys. B At. Mol. Opt. Phys.* **32**, 5289 (1999).
- [57] S. Bhattacharjee, C. Bagdia, M. R. Chowdhury, J. M. Monti, R. D. Rivarola, and L. C. Tribedi, *Eur. Phys. J. D* **72**, 15 (2018).
- [58] A. V. Verkhovtsev and A. V. Solov'yov (private communication).